

# A New Approach to the Fusion of EEG and MEG Signals Using the LCMV Beamformer

Hamid R. Mohseni<sup>\*§</sup>, Morten L. Kringelbach<sup>†§</sup>, Mark W. Woolrich<sup>‡</sup>, Tipu Z. Aziz<sup>§</sup> and Penny Probert Smith<sup>\*</sup>

<sup>\*</sup>Institute of Biomedical Engineering, School of Engineering Science, University of Oxford, Oxford, UK

<sup>†</sup>Department of Psychiatry, University of Oxford, Warneford Hospital, UK

<sup>‡</sup>Oxford Centre for Human Brain Activity, Department of Psychiatry, University of Oxford

<sup>§</sup>Oxford Functional Neurosurgery, Nuffield Department of Surgery, John Radcliffe Hospital, Headington, Oxford, UK

**Abstract**—In this paper, we demonstrate a new approach for the fusion of multichannel signals. We show how this method can be used to combine signals from magnetometer and gradiometer sensors used in magnetoencephalography (MEG). This approach works by assuming that the lead-fields have multiplicative errors which in turn leads to an under-determined problem. To solve this problem, we impose two constraints that result in closed-form solutions: i) one set of sensors is error-free, ii) the norm of the multiplicative error is bounded. These prior assumptions to estimate the error are used in the linearly constraint minimum variance (LCMV) spatial filter to improve the optimisation. Although we focus on the fusion of MEG sensors, this approach can be employed for multimodal fusion of other multichannel signals such as MEG and EEG signals.

**Index Terms**—LCMV beamformer, magnetoencephalography, magnetometer, gradiometer, sensor fusion

## I. INTRODUCTION

MEG is a non-invasive neuroimaging technique that is showing great promise in increasing our understanding of the functional activity of the human brain. It offers excellent temporal resolution on the scale of milliseconds, however, it suffers from poor spatial resolution.

There are two fundamental classes of MEG sensors known as *magnetometers* and *gradiometers*. In the ideal situation, the gradiometers and magnetometers measure simultaneously the same activity and should reveal the same neural activity. However, there are a number of studies that suggest the multimodal data sets have incommensurate measurement unit and suffer from different level of noise—magnetometers measure total flux (Tesla), while gradiometers measure a gradient (Tesla/meter). This means that combining two sensor types without any correction does not necessarily improve the spatial resolution of reconstructed sources, and one modality would dominate the other for example in the inverse of the covariance matrix [1]–[4]. Therefore, multimodal inversion requires some form of scaling that determines the relative contribution of each modality to the estimates of source activity. This scaling usually depends on the estimation of signal-to-noise ratio (SNR), whereby all sensors or sensor group signals are scaled according to their statistical significances. SNR can be estimated based on the intrinsic factory noise measurement (Max-Filter Users Guide, Version 2.0, Elekta Neuromag, Appendix B2), or on empirical estimates; e.g., from empty-room data, or pre-stimulus baseline periods. However, estimating the pure

sensor-level noise is sometimes intractable, and estimation of SNR from real data, which often use pre-stimulus baseline periods, may confuse sensor noise with endogenous neural activity [5]. An accurate and robust method to fuse of magnetometer and gradiometer to improve their joint estimation is therefore an important goal in improving MEG interpretation.

Amongst previous research in multimodal fusion of neuronal data, simultaneous recording and simple combination of MEG and EEG have been investigated [6]–[10]. In addition, there is a wide range of intelligent approaches for the fusion of MEG and EEG such as regularised linear inverse source estimation [11], independent component analysis [12], lead-field correction for dipolar sources [13], minimum  $l_2$  norm estimation [4], mutual information [14], Bayesian estimation [15] and the use of a neural mass model [16].

We propose a method, which is an extension of that we recently presented in [18], for the multimodal fusion of MEG sensors in the linearly constraint minimum variance (LCMV) beamformer framework (the beamformer is a spatial filter that minimises the power of the signal while passing the activity from the location of interest [17]). Since the proposed problem formulation is under-determined, prior assumptions are necessarily to solve this problem. Here, we investigate two different scenarios by which solutions that are closed form are obtained: one based on assuming one set of sensors is more accurate and the other based on joint normalisation of both sensor types. As discussed in the final section, these models are applicable under different imaging conditions.

## II. PROBLEM FORMULATION AND ITS TWO SOLUTIONS

Consider the following problem formulation:

$$\begin{aligned} y_g &= F_g E_g s + n_g \\ y_m &= F_m E_m s + n_m \end{aligned} \quad (1)$$

where  $y_g \in \mathbb{R}^{N_g \times T}$  and  $y_m \in \mathbb{R}^{N_m \times T}$  are measurements acquired using gradiometer and magnetometer sensors with the associated and known lead-fields  $F_g \in \mathbb{R}^{N_g \times D}$  and  $F_m \in \mathbb{R}^{N_m \times D}$ , respectively. In this formulation,  $E_g, E_m \in \mathbb{R}^{D \times D}$  are the multiplicative errors varying from location to location. Let also  $s \in \mathbb{R}^{D \times T}$  be the time course of the desired source, and  $n_g \in \mathbb{R}^{N_g \times T}$  and  $n_m \in \mathbb{R}^{N_m \times T}$  be the additive zero-mean Gaussian white noises.

Note that (1) can be rewritten as:

$$y = F_{gm}E_{gm}s + n \quad (2)$$

where  $y = \begin{bmatrix} y_g \\ y_m \end{bmatrix}$ ,  $F_{gm} = \begin{bmatrix} F_g & 0 \\ 0 & F_m \end{bmatrix}$ ,  $E_{gm} = \begin{bmatrix} E_g \\ E_m \end{bmatrix}$  and  $n = \begin{bmatrix} n_g \\ n_m \end{bmatrix}$ . It is assumed that  $y$  is a stationary zero-mean process with covariance matrix  $R_y$ , which is symmetric and positive definite. Our aim is to provide an accurate estimation of the multiplicative error  $E_{gm}$ .

$E_{gm}$  cannot be uniquely identified, because for a particular solution of  $s$ , all its linear transformations are also solutions. Here, therefore, we consider two different constraints to be able to solve this problem:

- i. One of  $E_g$  or  $E_m$  is known
- ii.  $E_{gm}^T E_{gm} = I$ , where  $I$  is the identity matrix

These assumptions lead to computationally tractable, fast and closed-form solutions. We will explore the impact of these assumptions in Section III.

The estimation of the multiplicative error  $E_{gm}$  can be found by considering the following modified LCMV beamformer (for details of the LCMV beamformer please refer to [17]):

$$\begin{aligned} \arg \min_W \arg \max_{E_{gm}} \text{Tr}\{W^T R_y W\} \\ \text{subject to: } W^T F_{gm} E_{gm} = I \end{aligned} \quad (3)$$

where  $R_y$  is the covariance matrix, and  $\text{Tr}\{\cdot\}$  and  $(\cdot)^T$  are trace and transpose operators, respectively. The solution is a linear filter  $W^T$  that minimises the output power when it has been maximised by the multiplicative error  $E_{gm}$ . This optimisation problem ensures the output power is minimised when the error has the worst effect, and thus guarantees the performance of the beamformer in all range of the errors.

To find the solution, first suppose that  $E_{gm}$  is known. Following methods used in [17],  $W$  can be estimated using the Lagrange multiplier method as:

$$W^T = (E_{gm}^T F_{gm}^T R_y^{-1} F_{gm} E_{gm})^{-1} F_{gm}^T E_{gm}^T R_y^{-1} \quad (4)$$

By putting (4) into the constraint in (3), it is clear that this estimate of  $W^T$  always satisfies the constraint for any choice of  $E_{gm}$ . As a result,  $E_{gm}$  can be estimated by only maximising the power  $\mathcal{P} = \text{Tr}\{W^T R_y W\}$ . Using (4), and some algebraic manipulation, the power is expressed as:

$$\mathcal{P} = \text{Tr}\{(E_{gm}^T F_{gm}^T R_y^{-1} F_{gm} E_{gm})^{-1}\} \quad (5)$$

Now we continue under constraint i. Without loss of generality we assume that  $E_g$  is known and suppose that  $E_g = I$  for simplification of notation. By partitioning the inverse of joint covariance matrix into  $R_y^{-1} = \begin{bmatrix} R_{gg}^- & R_{gm}^- \\ R_{mg}^- & R_{mm}^- \end{bmatrix}$ , equation (3) using (5) is expressed as:

$$\begin{aligned} \arg \max_{E_m} \mathcal{P} = \arg \max_{E_m} \text{Tr}\left\{ \left( E_m^T F_m^T R_{mm}^- F_m E_m + \right. \right. \\ \left. \left. E_m^T F_m^T R_{mg}^- F_g + F_g^T R_{gm}^- F_m E_m + F_g^T R_{gg}^- F_g \right)^{-1} \right\} \end{aligned} \quad (6)$$

The derivative of the above expression with respect to  $E_m$  is equal to:

$$\begin{aligned} \frac{\partial \mathcal{P}}{\partial E_m} = - \left( E^T F_m^T R_{mm}^- F_m E_m + E_m^T F_m^T R_{mg}^- F_g + \right. \\ \left. F_g^T R_{gm}^- F_m E_m + F_g^T R_{gg}^- F_g \right)^{-2} \\ \left( 2E_m^T F_m^T R_{mm}^- F_m + (F_m^T R_{mg}^- F_g)^T + F_g^T R_{gm}^- F_m \right) \end{aligned} \quad (7)$$

Since the expression inside the first bracket is invertible, its inverse is full rank and the above expression is only zero if the expression inside the second bracket is zero. Hence, the problem in (6) is convex and the global maximum, using the fact that  $F_m^T R_{mg}^- F_g = (F_g^T R_{gm}^- F_m)^T$ , is given by:

$$E_m = -(F_m^T R_{mm}^- F_m)^{-1} (F_m^T R_{mg}^- F_g) \quad (8)$$

Equation (8) also can be rewritten as:

$$E_m = -(F_{om}^T R_y^{-1} F_{om})^{-1} (F_{om}^T R_y^{-1} F_{go}) \quad (9)$$

where  $F_{om} = \begin{bmatrix} 0 \\ F_m \end{bmatrix}$  and  $F_{go} = \begin{bmatrix} F_g \\ 0 \end{bmatrix}$ . Therefore the above equation is the solution under constraint i.

Now we continue under constraint ii. By defining  $C_{gm} = F_{gm}^T R^{-1} F_{gm}$  and using equation (5), we have the following optimisation problem:

$$\begin{aligned} \arg \max_{E_{gm}} \text{Tr}\{(E_{gm}^T C_{gm}^{-1} E_{gm})^{-1}\} \\ \text{subject to: } E_{gm}^T E_{gm} = I \end{aligned} \quad (10)$$

This is solved using its Lagrangian which is:

$$\mathcal{L}(E_{gm}, \Gamma) = \text{Tr}\{(E_{gm}^T C_{gm}^{-1} E_{gm})^{-1} + E_{gm}^T E_{gm} \Gamma - \Gamma\} \quad (11)$$

where  $\Gamma$  is the Lagrange multiplier. Then, the derivative of (11) is expressed as:

$$\frac{\partial \mathcal{L}(E_{gm}, \Gamma)}{\partial E_{gm}} = 2(E_{gm}^T C_{gm} E_{gm})^{-2} E_{gm}^T C_{gm} - 2\Gamma E_{gm}^T \quad (12)$$

By equalling the above equation to zero and defining  $\tilde{\Gamma} = (E_{gm}^T C_{gm}^{-1} E_{gm})^2 \Gamma$ , we have:

$$E_{gm}^T C_{gm}^{-1} = \tilde{\Gamma} E_{gm}^T \quad (13)$$

Note that because  $E_{gm}^T C_{gm}^{-1} E_{gm}$  is invertible which means for any  $\Gamma$  there is a unique  $\tilde{\Gamma}$ . Therefore, the above equation results in  $E_{gm}^T = US$ , where  $U$  is an arbitrary orthonormal matrix and  $S$  is the eigenvector matrix of  $C_{gm}^{-1}$  or equivalently  $C_{gm}$ . Since this  $E_{gm}$  should maximise the first expression in (10), it can be inferred that *the solution for  $E_{gm}$  under constraint ii. is constructed by the eigenvectors of  $C_{gm}$  corresponding to the  $D$  smallest eigenvalues.* It is clear that any linear transformation of this  $E_{gm}$  under an orthonormal matrix is a solution as well.

### III. SIMULATION EXPERIMENT

To investigate the advantages and disadvantages of each method, MEG data with Gaussian sources were simulated. The number of sources were set to 15 and the number of sensors for

each sensor type to 102. The sources were non-correlated and their lead-fields were chosen randomly in a Monte Carlo like simulation; i.e. the location of sensors and sources were chosen randomly. We set  $D = 2$ , and elements of the multiplicative errors  $E_g$  and  $E_m$ , were chosen independently in each Monte Carlo simulation according to a uniform random distribution in the range of 0 to 1. Gaussian white noise was added to the signal after applying the lead-field to the time series of the sources. The following results were produced as the average of 1000 Monte Carlo simulations. MSE is the mean squared error between original and estimated time course which were normalised by their power. This normalisation effectively means that the amplitude of time series can be ignored.

Fig. 1 and 2 show the MSE of the methods versus SNR which is defined in the sensor space as the ratio of the mean power of the signal of interest across the sensors (applying the lead-field only to the source of interest) to the mean power of the added noise also across the sensors. In these figures, the label ‘fuse’ indicates when the constraint  $E_{gm}^T E_{gm} = I$  were used to fuse the sensors. The results labelled ‘fuse-grad’ and ‘fuse-mag’ correspond to the fusion methods with a correct lead-field assumed for gradiometer ( $E_g = I$ ) and magnetometer ( $E_m = I$ ), respectively. The results labelled ‘grad’ and ‘mag’ show the results from using only the gradiometer sensor or the magnetometer sensor, respectively.

Fig. 1 shows the MSE versus SNR of the Monte Carlo simulation using  $E_g = I$  (i.e. when the gradiometer is error-free) and the multiplicative error of the magnetometer  $E_m$  is randomly varying from simulation to simulation. These assumptions are comparable to the ‘fuse-grad’ method and as expected, it shows smaller MSE compared to others. Similarly, the ‘grad’ method shows better performance than ‘fuse-grad’ for the obvious reason that the gradiometer is error-free. The ‘fuse’ method, which uses the modified lead-fields, outperforms both ‘mag’ and ‘fuse-mag’ methods, since the assumption that is used to simulate the data is against their underlying assumption.

Fig. 2 demonstrates the results when both sensor types have the multiplicative errors. The ‘fuse’ method has the best performance since its assumptions better match the assumptions used in the simulation. The ‘fuse-grad’ and ‘fuse-mag’ outperform the single modality approaches because they use a larger number of sensors to reconstruct the same number of sources.

#### IV. REAL DATA RESULTS

Some studies suggest that a specific region of the brain, the fusiform face area (FFA), is the primary face processing region in the human brain [19]–[21]. The FFA is a part of the human visual system and located within the fusiform cortex above the cerebellum. Various studies using MEG and EEG have demonstrated that face-specific components in the brain signals peak at approximately 170ms after presentation of the face [22], [23]. This face-specific components have become known as the M170 in MEG studies and appear to

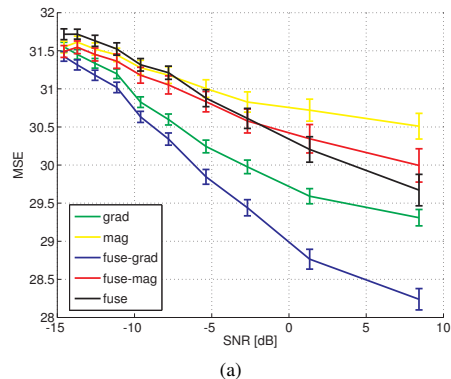


Fig. 1: Comparing signal-to-noise (SNR) and MSE (mean squared error) when  $E_g = I$  and the elements of  $E_m$  are randomly chosen according to a uniform distribution.

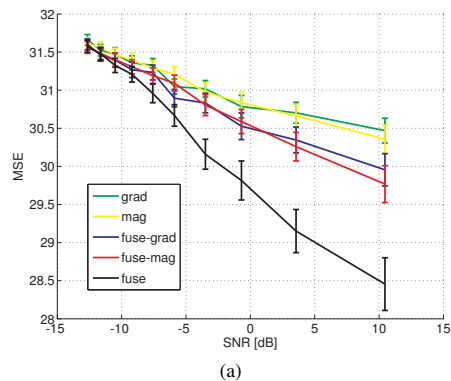


Fig. 2: Comparing signal-to-noise (SNR) and MSE (mean squared error) when the elements of  $E_g$  and  $E_m$  are randomly chosen according to a uniform distribution.

be significantly earlier and larger for faces than other objects in the FFA.

In this experiment a series of animal and human faces were presented to the participants. Each image were presented for 300ms and the time interval between images was 1500ms. The sampling rate was 1kHz and after linearly filtering data in the range of 1–40Hz the recorded data were epoched and averaged for animal and human faces. MaxFilter, a filtering package to remove spurious signals, were used to further denoise the data (MaxFilter Users Guide, Version 2.0, ELEKTA neuromag). The trials were visually inspected and few of them with large variations were removed. The differences between MEG signals for human and animal faces from 150ms to 190ms after stimuli were used to estimate the covariance matrix. The covariance matrix was diagonally regularised with 5% of its trace. A single layer realistic head model was used in which the brain was divided into a number of cells. The distance between adjacent cells was 5mm. The power of the beamformer at each cell was computed and normalised with those of the noise estimated from the pre-stimulus trials.

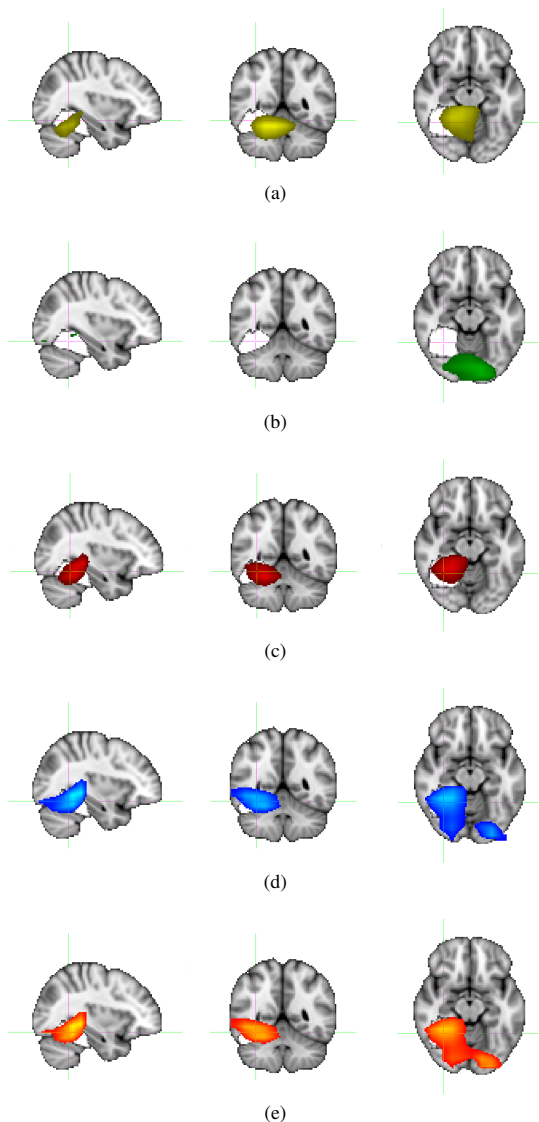


Fig. 3: Localising the face response by using the normalised estimated output power of beamformer using (a) ‘mag’, (b) ‘grad’, (c) ‘fuse-mag’, (d) ‘fuse-grad’, (e) and ‘fuse’ methods. The solid white volume is the extent of the fusiform cortex within which there are regions of neurons with face specific responses.

Fig. 3 shows the output power (trace of estimated covariance matrix as in equation (5)) of the beamformer normalised by norm of the associated lead-fields; i.e. normalised by the power of projected Gaussian white noise (see [17]). The reconstructed activity was thresholded using the normalised threshold of 90%. The same anatomical plane is displayed for each method. In all the figures the solid white volume is the mask representing the full fusiform cortex region depicted using the automated anatomical labelling (AAL) atlas, within which the FFA can be found [24].

Fig. 3(a) shows the results using ‘mag’, where the peak of the power spectrum is close to the FFA area, but it is biased towards the mid-line. Fig. 3(b) shows the results using ‘grad’, where the peak of power spectrum is close to the visual cortex and away from FFA. Figs. 3(c) and (d) show the results from ‘fuse-mag’ and ‘fuse-grad’, respectively. Both methods show better performance than the results in Figs. 3(a) and (b), as seen from the greater overlap between the source and FFA. However, they show some difference in the source activity detected in the visual cortex (Fig. 3(c) axial view). It is notable that there is similarity between the results of ‘fuse-grad’ and ‘grad’, and between ‘fuse-mag’ and ‘mag’ method. Fig. 3(e) shows the results from ‘fuse’ method. This method also reconstructed the FFA correctly. The results are similar to the ‘fuse-grad’ method with slightly larger activity in the visual cortex.

## V. DISCUSSION AN CONCLUSIONS

We proposed a novel method for the multimodal fusion of magnetometer and gradiometer in MEG imaging. In this method the LCMV spatial filter is modified, and its closed-form solutions were obtained using two prior assumptions.

Based on the simulations and real data, we may conclude that the fusion methods can improve the results of using single modality methods. However in a real application a choice between the methods must be determined. This may be done as follows. First note that for the moderate noisy signals, the choice does not have great impact on the final results. Second, it is dependent on the available data set, for example, employing ‘fuse-grad’ method generally seems more appropriate than the others, since the gradiometer suffer from less noise and have twice number of sensors compared to the magnetometer. In addition, The ‘fuse-mag’ method might be preferred for deep sources, since magnetometers are more sensitive in this region. On the other hand, if there is no prior information about whether to choose one modality over another, the ‘fuse’ method is likely to yield the best results.

Further work is needed in this area to find a reliable way to determine the best way to select or combine the different fusion methods.

## ACKNOWLEDGMENT

This work is funded by the Wellcome Trust and EPSRC under grant number WT 088877/Z/09/Z.

## REFERENCES

- [1] R. E. Greenblatt, *Combined EEG/MEG source estimation methods*, C. Baumgartner, L. Deecke, G. Stroink, and S. J. Williamson, Eds. Elsevier, 1995.
- [2] M. Fuchs, M. Wagner, H. A. Wischmann, T. Kohler, A. Theissen, R. Drenckhan, and H. Buchner, “Improving source reconstructions by combining bioelectric and biomagnetic data,” *Electroencephalogr. Clin. Neurophysiol.*, vol. 107, 1998.
- [3] F. H. Lin, Belliveau, J. W., Dale, A. M., and M. Hamalainen, “Distributed current estimates using cortical orientation constraints,” *Hum. Brain Mapp.*, vol. 27, pp. 1–13, 2006.
- [4] A. Molins, S. M. Stufflebeam, E. N. Brown, and M. S. Hamalainen, “Quantification of the benefit from integrating MEG and EEG data in minimum l2-norm estimation,” *NeuroImage*, vol. 42, no. 3, pp. 1069–1077, 2008.

- [5] R. N. Henson, E. Mouchlianitis, and K. J. Friston, "MEG and EEG data fusion: Simultaneous localisation of face-evoked responses," *NeuroImage*, vol. 47, no. 2, pp. 581–589, 2009.
- [6] C. Wood, D. Cohen, B. Cuffin, M. Yarita, and T. Allison, "Electrical sources in human somatosensory cortex: identification by combined magnetic and potential recordings," *Science*, vol. 227, no. 4690, pp. 1051–1053, 1985.
- [7] W. W. Sutherling, P. H. Crandall, T. M. Darcey, D. P. Becker, M. F. Levesque, and D. S. Barth, "The magnetic and electric fields agree with intracranial localizations of somatosensory cortex," *Neurol.*, vol. 38, pp. 1705–1714, 1988.
- [8] A. M. Dale and M. I. Sereno, "Improved localization of cortical activity by combining EEG and MEG with MRI cortical surface reconstruction: A linear approach," *J. Cogn. Neurosci.*, vol. 5, pp. 162–176, 1993.
- [9] J. Phillips, R. Leahy, J. Mosher, and B. Timsari, "Imaging neural activity using MEG and EEG," *Engineering in Medicine and Biology Magazine, IEEE*, vol. 16, no. 3, pp. 34–42, 1997.
- [10] F. Babiloni, D. Mattia, C. Babiloni, L. Astolfi, S. Salinari, A. Basilisco, P. M. Rossini, M. G. Marciani, and F. Cincotti, "Multimodal integration of EEG, MEG and fMRI data for the solution of the neuroimage puzzle," *Magnetic Resonance Imaging*, vol. 22, no. 10, pp. 1471–1476, 2004.
- [11] F. Babiloni, F. Carducci, F. Cincotti, C. Del Gratta, V. Pizzella, G. L. Romani, P. M. Rossini, F. Tecchio, and C. Babiloni, "Linear inverse source estimate of combined EEG and MEG data related to voluntary movements," *Human Brain Mapping*, vol. 14, no. 4, pp. 197–209, 2001.
- [12] H. Zavala-Fernandez, T. H. Sander, M. Burghoff, R. Orglmeister, and L. Trahms, "Multi-modal ICA exemplified on simultaneously measured MEG and EEG data," in *Proceedings of the 7th international conference on Independent component analysis and signal separation*, ser. ICA'07. Berlin, Heidelberg: Springer-Verlag, 2007, pp. 673–680.
- [13] M.-X. Huang, T. Song, D. J. H. Jr., I. Podgorny, V. Jousmaki, L. Cui, K. Gaa, D. L. Harrington, A. M. Dale, R. R. Lee, J. Elman, and E. Halgren, "A novel integrated MEG and EEG analysis method for dipolar sources," *NeuroImage*, vol. 37, no. 3, pp. 731–748, 2007.
- [14] S. Baillet, L. Garnero, G. Marin, and J.-P. Hugonin, "Combined MEG and EEG source imaging by minimization of mutual information," *Biomedical Engineering, IEEE Transactions on*, vol. 46, no. 5, pp. 522–534, 1999.
- [15] S. C. Jun, "MEG and EEG fusion in bayesian frame," in *Electronics and Information Engineering (ICEIE), 2010 International Conference On*, vol. 2, 2010, pp. V2–295–V2–299.
- [16] A. Babajani-Feremi and H. Soltanian-Zadeh, "Multi-area neural mass modeling of EEG and MEG signals," *NeuroImage*, vol. 52, no. 3, pp. 793–811, 2010.
- [17] B. Van Veen, W. Van Drongelen, M. Yuchtman, and A. Suzuki, "Localization of brain electrical activity via linearly constrained minimum variance spatial filtering," *Biomedical Engineering, IEEE Transactions on*, vol. 44, no. 9, pp. 867–880, 1997.
- [18] "Fusion of magnetometer and gradiometer sensors of MEG in the presence of multiplicative error." *IEEE transactions on bio-medical engineering*, vol. 59, no. 7, pp. 1951–61, Jul. 2012.
- [19] J. SERGENT, "Functional neuroanatomy of face and object processing," *Brain*, vol. 115, pp. 15–36, 1992.
- [20] N. Kanwisher, J. McDermott, and M. M. Chun, "The fusiform face area: A module in human extrastriate cortex specialized for face perception," *The Journal of Neuroscience*, vol. 17, no. 11, pp. 4302–4311, 1997.
- [21] E. Halgren, T. Raij, K. Marinkovic, V. Jousmaki, and R. Hari, "Cognitive response profile of the human fusiform face area as determined by MEG," *Cerebral Cortex*, vol. 10, no. 13, pp. 69–81, 2000.
- [22] I. Deffke, T. Sander, J. Heidenreich, W. Sommer, G. Curio, L. Trahms, and A. Lueschow, "MEG/EEG sources of the 170-ms response to faces are co-localized in the fusiform gyrus," *NeuroImage*, vol. 35, no. 4, pp. 1495–1501, 2007.
- [23] J. Liu, A. Harris, and N. Kanwisher, "Stages of processing in face perception: an MEG study," *Nature Neuroscience*, vol. 5, pp. 910–916, 2002.
- [24] N. Tzourio-Mazoyer, B. Landeau, D. Papathanassiou, F. Crivello, O. Etard, N. Delcroix, B. Mazoyer, and M. Joliot, "Automated anatomical labeling of activations in spm using a macroscopic anatomical parcellation of the mni mri single-subject brain," *NeuroImage*, vol. 15, no. 1, pp. 273–289, 2002.